Studies of quantum dots

Fei Yuan,[1] Sarah Reimann,[2] Scott Bogner,[1] and Morten Hjorth-Jensen[1,3]

[1] *National Superconducting Cyclotron Laboratory and Department of Physics and Astronomy, Michigan State University, East Lansing, MI 48824, USA*

[2] *Department of Chemistry and Center for Theoretical and Computational Chemistry, University of Oslo, N-0316 Oslo, Norway*

[3] *Department of Physics, University of Oslo, N-0316 Oslo, Norway*

We present and compare several many-body methods used to study a quantum dot system. We calculate the approximate ground state energy of electrons in a circularly symmetric potential well using a harmonic oscillator basis optimized via Hartree-Fock. We further improve the ground state energy using in-medium similarity renormalization group (IM-SRG). Additionally, we calculate the addition and removal energies using quasidegenerate perturbation theory (QDPT). Our results are benchmarked against quasi-exact diffusion Monte Carlo results from previous works. Possible explanations for the discrepancies are discussed.

PACS numbers: 02.70.Ss, 31.15.A-, 31.15.bw, 71.15.-m, 73.21.La

I. INTRODUCTION

Understanding the behaviour of strongly confined electrons is of fundamental interest for solving many-body problems. Quantum dots, e.g. electrons confined in semiconducting heterostructures, are of particular interest since they exhibit, due to their small size, discrete quantum levels. Under these conditions, typical quantum phenomena like tunnelling, entanglement and magnetization can all be observed [1, 2]. Since quantum dots are manufactured and designed artificially at the laboratory, their quantum levels can be tuned to one's needs by changing for instance the external field, or the size and shape of the system. As a consequence, quantum dots provide a high level of control for the dynamics and correlation of the electrons, which makes them perfectly suited to study quantum effects in practice. Since their ground state shows similar shell structures and magic numbers as seen for atoms and nuclei [3], these systems give the opportunity to study electronic systems without the presence of a nucleus affecting the electrons. Apart from their relevance for theoretical research in quantum physics, quantum dots offer a wide variety of applications: In particular, their electrical and optical properties make them attractive for the use in laser technology [4, 5] and solar cells [6, 7], but they are also used in quantum computers [8] and medical imaging [9].

In order to properly understand the properties of quantum dots and make theoretical predictions to their behaviour in various applications, it is necessary to study features like ground state energy and correlation effects. Since apart from quantum dots consisting of only two electrons or with specific values of the external field, no analytical solutions exist [10], the development of appropriate few- and many-body methods is required.

Several *ab initio* methods have been applied to these systems, in particular variational and diffusion Monte Carlo [11–14], large-scale diagonalization [15–18] and Coupled Cluster theory [13, 19, 20].

Additionally to those approaches, another very promising first-principle method has recently evolved. This is the Similarity Renormalization Group (SRG) method, which drives the Hamiltonian to a band- or block-diagonal form using a continuous series of unitary transformations. Especially in nuclear theory, it has successfully been applied to study systems with different underlying potentials, and it has been used to analyse their binding energy and other observables [21–23]. Apart from the free-space approach, where the Hamiltonian is set up with respect to the zero vacuum state, in recent times another interesting alternative has been worked out: Making use of the technique of normal-ordering, the SRG evolution is performed in medium, where 3, ..., A-body operators can be approximated using only two-body machinery. This in-medium SRG (IM-SRG) allows considerable simplifications to the problem and makes numerical calculations much more efficient [24].

This article is organized as follows: Section II introduces first (II A) the Hamiltonian we use to model circular quantum dots, and gives afterwards an overview over the SRG (**??**) and DMC (**??**) formalism. Our results are presented in Section III. We point out the differences arising from the use of two different generators, Wegner's and White's one, and give an overview over the ground state energies up to 42 particles. In particular, we compare the results obtained with five different *ab initio* methods: IM-SRG(2), DMC, Hartree-Fock, Full Configuration Interaction and Coupled Cluster. Section IV concludes our work and gives perspectives for future work.

The harmonic oscillator (HO) is ubiquitous in quantum physics. It is the basis for extremely diverse many-body calculations in nuclear physics,[**?**] quantum chemistry,[**?**] and quantum dot calculations in solid state physics.[**?**] In these calculations, one typically seeks a few of the lowest eigenenergies E_k of the system Hamiltonian H, and their corresponding eigenvectors ψ_k, viz,

$$H\psi_k = E_k\psi_k, \quad k = 1, \cdots, k_{\max}.$$

In all cases, the many-body wave function is expanded in a basis of eigenfunctions of the HO, and then necessarily

truncated to give an approximation. In fact, the so-called curse of dimensionality implies that the number of degrees of freedom per particle available is severely limited. It is clear, that an understanding of the properties of such expansions, giving *a priori* error estimates on many-body calculations, is very important. Unfortunately, this is a neglected topic in the physics literature. In this article, we give a thorough mathematical and numerical analysis and give practical convergence estimates of HO basis expansions. It generalizes and refines the findings of a recent study of one-dimensional systems.[**?**]

The HO eigenfunctions are popular for several reasons. Many quantum systems, such as the quantum dot model considered here, are perturbed harmonic oscillators *per se*, so that the true eigenstates should be perturbations of the HO states. Moreover, the HO has many beautiful properties, such as separability, invariance under orthogonal coordinate changes, and easily computed eigenfunctions, so that computing matrix elements of relevant operators becomes relatively simple. The HO eigenfunctions are defined on the *whole* of $\mathbb{R}^d$ in which the particles live, so that truncation of the domain is unnecessary. Indeed, this is one of the main problems with methods such as finite difference or finite element methods.[**?**]

II. FORMALISM

A. The model Hamiltonian

We model the quantum dot as a collection of N electrons trapped in an external harmonic-oscillator potential.[1] Each electron possesses kinetic energy $t(\boldsymbol{p}) \equiv \boldsymbol{p}^2/2$ and experiences an external potential

$$u(\boldsymbol{r}) \equiv \frac{1}{2}\omega^2 \boldsymbol{r}^2$$

where ω is the angular frequency of the oscillator, $\boldsymbol{r}$ is the 2-dimensional coordinate of an electron, and $\boldsymbol{p}$ is its momentum. Each pair of electrons experience a Coulomb repulsion

$$v(\boldsymbol{r}, \boldsymbol{r}') \equiv \frac{1}{|\boldsymbol{r} - \boldsymbol{r}'|}$$

where $\boldsymbol{r}$ and $\boldsymbol{r}'$ are coordinates of a pair of electrons. Thus, the full many-body problem is described by the nonrelativistic Hamiltonian

$$\hat{H} \equiv \sum_p \big(t(\hat{\boldsymbol{p}}_p) + u(\hat{\boldsymbol{r}}_p)\big) + \sum_{\{p,q\}} v(\hat{\boldsymbol{r}}_p, \hat{\boldsymbol{r}}_q)$$

where $\hat{\boldsymbol{p}}_p$ is the momentum operator and $\hat{\boldsymbol{r}}_p$ is the position operator for a particle labeled by p. The first summation is performed over every particle p, while the the second summation is performed over every unordered pair of particles $\{p, q\}$ (with $p \neq q$).

The full problem is not a trivial one. We shall first consider a much simpler problem: a noninteracting Hamiltonian $\hat{H}^{\mathrm{o}}$ in which the Coulomb interaction v is removed:

$$\hat{H}^{\mathrm{o}} \equiv \sum_p \big(t(\hat{\boldsymbol{p}}_p) + u(\hat{\boldsymbol{r}}_p)\big)$$

In this case, the many-body Hamiltonian reduces to N independent single-particle Hamiltonians, each of the form:

$$\hat{h}^{\mathrm{o}} \equiv \frac{\hat{\boldsymbol{p}}^2 + \omega^2 \hat{\boldsymbol{x}}^2}{2}$$

This is a 2-dimensional harmonic oscillator problem for a single particle, whose solutions are well known. There are, however, various ways to construct the set of eigenfunctions: we shall use the Fock-Darwin states that conserve angular momentum about the axis perpendicular to the plane. The eigenfunctions have the following analytic form in polar coordinates:[25, Appx. A]

$$\phi^{\mathrm{fd}}_{n,m_\ell}(r, \varphi) \equiv \sqrt{\omega}\phi^{\mathrm{fdr}}_{n,|m_\ell|}(\sqrt{\omega}r)\phi^{\mathrm{fda}}_{m_\ell}(\varphi)$$

where

$$\phi^{\mathrm{fdr}}_{n,\mu}(\rho) \equiv \sqrt{\frac{2 \cdot n!}{(n+\mu)!}} \mathrm{e}^{-\rho^2/2} \rho^\mu L^{(\mu)}_n(\rho^2)$$

$$\phi^{\mathrm{fda}}_{m_\ell}(\varphi) \equiv \frac{1}{\sqrt{2\pi}} \mathrm{e}^{i m_\ell \varphi}$$

and $L^{(\mu)}_n$ denotes the generalized Laguerre polynomial of degree n with parameter μ. The states are labelled by two quantum numbers: the principal quantum number $n \in \{0, 1, \ldots\}$ and the angular momentum projection $m_\ell \in \mathbb{Z}$.

Additionally, since electrons are spin-1/2 fermions, they can occupy either of the two spin states $\chi_{+\frac{1}{2}}$ or $\chi_{-\frac{1}{2}}$. Thus, the single-particle basis states can be constructed as

$$\phi_{n,m_\ell,m_{\mathrm{s}}}(r, \varphi) \equiv \phi^{\mathrm{fd}}_{n,m_\ell}(r, \varphi)\chi_{m_{\mathrm{s}}} \tag{1}$$

with the spin projection $m_{\mathrm{s}} \in \left\{-\frac{1}{2}, +\frac{1}{2}\right\}$.

The eigenvalues of the single-particle Hamiltonian $\hat{h}^{\mathrm{o}}$ are given by

$$\varepsilon_{n,m_\ell,m_{\mathrm{s}}} \equiv (2n + |m_\ell| + 1)\omega$$

Note that they are degenerate with respect to the spin projection m_{s} since our Hamiltonian $\hat{h}^{\mathrm{o}}$ does not distinguish between them. From this equation, we can see that the single-particle basis states form a shell structure as shown in Figure 1. Every state within a given shell is degenerate and states within a given shell satisfy

[1] In this paper, we use atomic units where $\hbar$, m, e, and $4\pi\epsilon$ are unity, with ϵ denoting the permittivity and m denoting the mass, which may be an effective mass. In vacuum where $m = m_{\mathrm{e}}$ and $\epsilon = \epsilon_0$, energy would be measured in units of hartrees $E_{\mathrm{h}} \equiv m_{\mathrm{e}}(\alpha c)^2$. More generally, the units of energy are $m_{\mathrm{r}}E_{\mathrm{h}}/\epsilon_{\mathrm{r}}^2$ where $\epsilon_{\mathrm{r}} \equiv \epsilon/\epsilon_0$ and $m_{\mathrm{r}} \equiv m/m_{\mathrm{e}}$.

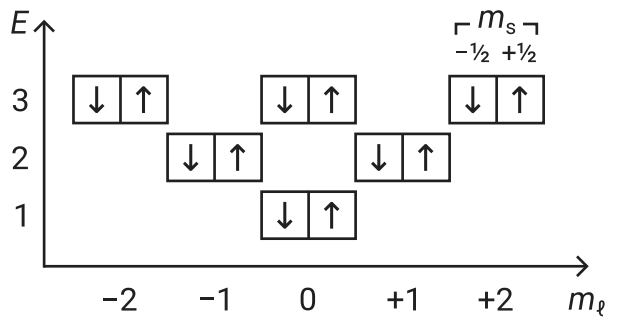

FIG. 1. Structure of the single-particle states in a noninteracting harmonic oscillator.

$2n + |m_\ell| = k$ for some nonnegative integer k, which we call the *shell index*. The shells are equidistant from each other, with a spacing equal to the frequency ω.

The many-body Hamiltonian $\hat{H}^{\mathrm{o}}$ is the sum of the single-particle Hamiltonians $\hat{h}_p^{\mathrm{o}}$ over all particles p, where p may now be treated as a tuple of all three single-particle quantum numbers: $(n, m_\ell, m_\mathrm{s})$. From the states ϕ in (1) we can construct the eigenstates of the many-body Hamiltonian $\hat{H}^{\mathrm{o}}$ in the form of Slater determinants that automatically satisfy the Pauli exclusion principle:

$$\Phi_{p_1,\ldots,p_N}(\boldsymbol{r}_1,\ldots,\boldsymbol{r}_N) \equiv \frac{1}{\sqrt{N}} \begin{vmatrix} \phi_{p_1}(\boldsymbol{r}_1) & \cdots & \phi_{p_N}(\boldsymbol{r}_1) \\ \vdots & \ddots & \vdots \\ \phi_{p_1}(\boldsymbol{r}_N) & \cdots & \phi_{p_N}(\boldsymbol{r}_N) \end{vmatrix}$$

The energy of these states is given by the sum of the single-particle energies:

$$E^{\mathrm{o}}_{p_1,\ldots,p_N} \equiv \varepsilon_{p_1} + \cdots + \varepsilon_{p_N}$$

For ground states, we may have degeneracies due to the shell structure of the single-particle basis. However, if $N = k_\mathrm{f}(k_\mathrm{f}+1)$ for some nonnegative integer k_f, there are just enough particles to form a closed-shell system. In this case, there is a unique, well-isolated ground state. The values of N for which this occurs are typically referred to as *magic numbers* and we call k_f the *number of filled shells*. This completes the solution of the noninteracting problem.

The difficulty in solving the full Hamiltonian $\hat{H}$ stems from the fact that the exact solution cannot be expressed in terms of a single Slater determinant due to the presence of interactions. Hence, it is not possible to reduce the problem to that of a single particle as we had done previously.

However, if we assume that the interaction alters the behavior of the system only mildly, we can use the Slater determinants of the noninteracting system as an initial guess for the solution, and then apply iterative methods to improve the accuracy of the solution.

Since Slater determinants are rather cumbersome to write out in full, we shall instead work in the more convenient formalism of second quantization:

$$|\Phi_{p_1,\ldots,p_N}\rangle = \hat{a}^\dagger_{p_1} \cdots \hat{a}^\dagger_{p_N} |\varnothing\rangle$$

Here, $\hat{a}^\dagger_p$ is the creation operator for the single-particle state p and $|\varnothing\rangle$ is the (true) vacuum state that is devoid of particles. Analogously, $\hat{a}_p$ is the annihilation operator for the state p.

Operators can be rewritten in this formalism as well. The one-body kinetic energy operator, defined by

$$\hat{T} \equiv \sum_p \hat{t}(\hat{\boldsymbol{p}}_p)$$

can be rewritten in second quantization as

$$\hat{T} = \sum_{p,q} T_{p,q} \hat{a}^\dagger_p \hat{a}_q$$

where the operator matrix element $T_{p,q} \equiv \langle \Phi_p | \hat{T} | \Phi_q \rangle$. This can likewise be extended for both $\hat{U}$ and $\hat{V}$,

$$\hat{U} = \sum_{p,q} U_{p,q} \hat{a}^\dagger_p \hat{a}_q$$
$$\hat{V} = \frac{1}{4} \sum_{p,q,r,s} V_{p,q,r,s} \hat{a}^\dagger_p \hat{a}^\dagger_q \hat{a}_s \hat{a}_r$$

where $U_{p,q} \equiv \langle \Phi_p | \hat{U} | \Phi_q \rangle$ and $V_{p,q,r,s} \equiv \langle \Phi_{p,q} | \hat{V} | \Phi_{r,s} \rangle$. Note that due to the antisymmetry present in the Slater determinants, we have the property that exchanging either p with q or r with s causes $V_{p,q,r,s}$ to reverse in sign.

B. Hartree-Fock method

The first correction that we will apply to our solution is that of the Hartree-Fock method. Using the variational principle, we compute an approximate ground state Ψ^{hf} by minimizing the energy

$$E^{\mathrm{hf}} \equiv \langle \Psi^{\mathrm{hf}} | \hat{H} | \Psi^{\mathrm{hf}} \rangle$$

with respect to Ψ^{hf}, subject to the restriction that Ψ^{hf} is a single Slater determinant constructed from a set of N orthonormal single-particle states. We denote each state ψ_u, where u is its label.

To make this computationally feasible, we further assume that the unknown states ψ are built from a linear combination of known functions, drawn from a finite set. This reduces the problem from an abstract mathematical one to a numerical linear algebra problem, with the caveat that this set of known functions must be chosen carefully.

Assuming the interaction is not too strong, we can use the single-particle states ϕ of our noninteracting Hamiltonian as a basis for the unknown states ψ. The two sets of states are then related by a linear transformation $\boldsymbol{C}$:

$$\psi_u \equiv \sum_p \phi_p C_{p,u}$$

To ensure the orthonormality of the states, we expand the set of unknown states ψ to have as many elements as the set of ϕ and require the *coefficient matrix* $\boldsymbol{C}$ to be unitary. While these conditions are more strict than necessary, they greatly simplify the calculations and the additional states are essential inputs for methods beyond Hartree-Fock. The set of states ψ now consists of N *occupied* states that participate in the Slater determinant Ψ^{hf} and the remaining *unoccupied* states that do not.

Since the coefficient matrix uniquely determines the unknown states, the variational problem has been reduced to that of solving of the coefficients $\boldsymbol{C}$ that minimize the energy E, which is given by

$$E^{\mathrm{hf}} = \sum_{\underline{u}} C^*_{p,u} H^{\mathrm{o}}_{p,q} C_{q,u} + \sum_{\underline{u},\underline{v}} C^*_{p,u} C^*_{q,u} V_{p,q,r,s} C_{r,u} C_{s,u}$$

where the underlined indices indicate that the summation is over occupied states only.

Using the method of Lagrange multiplers, the minimization problem can be reduced to the solving of a nonlinear equation – the *Hartree-Fock equation*:

$$\boldsymbol{f}\boldsymbol{C} = \boldsymbol{C}\boldsymbol{\epsilon} \tag{2}$$

where the *Fock matrix* $\boldsymbol{f}$ is defined as

$$f_{p,r} \equiv H^{\mathrm{o}}_{p,r} + \sum_{\underline{u}qs} C^*_{q,u} V_{p,q,r,s} C_{s,u} \tag{3}$$

and $\boldsymbol{\epsilon}$ is a vector of Lagrange multipliers with each element ϵ_u associated with a particular state u. While the Fock matrix $\boldsymbol{f}$ may appear to be an artificial Hamiltonian derived purely from the minimization problem, it can be generalized as an operator whose relevance extends beyond Hartree-Fock.

The Hartree-Fock equation can be solved by an iterative technique: a solution $\boldsymbol{C}$ can be fed into (3) and new solution can then obtained by solving the eigenvalue problem in (2) using the Fock matrix obtained. For the initial guess, we use the ground state of our noninteracting Hamiltonian, thus $\boldsymbol{C}$ is initially the identity matrix.

Since Hartree-Fock method restricts the ground state to a Slater determinant of single-particle states, it cannot provide an exact solution to a problem where correlation is present, even if the basis ϕ is infinite. The energy difference between the best Hartree-Fock energy and the exact ground state energy is thus by definition known as the *correlation energy*. There are various methods of recovering (at least parts of) this missing energy. The focus of this paper shall be on the IM-SRG method.

C. The IM-SRG method

In the similarity renormalization group (SRG) method, one performs a continuous sequence of unitary transformations on a Hamiltonian operator $\hat{H}$ to evolve it into a more "amenable" form – which generally implies decoupling a small model space of interest from its complement. The sequence is parameterized by a continuous variable s known as the *flow parameter*, which by convention we define to be 0 at the beginning of the sequence. Upon reaching s, the transformed Hamiltonian is given by

$$\tilde{H}(s) \equiv \hat{U}(s)\hat{H}\hat{U}(s)$$

where $U(s)$ describes the product of all such transformations since $s = 0$. At every step s', the differential unitary transformation is described by the exponential of an antihermitian operator $\eta(s)$, known as the *generator* of the transformation. When "integrated" as a product, the full transformation $\hat{U}(s)$ is recovered:[2]

$$\hat{U}(s) = \lim_{\Delta s' \to 0} \prod_{s'=0}^{s'=s} \mathrm{e}^{\hat{\eta}(s')\Delta s'}$$

The evolution of the Hamiltonian itself is governed by a differential equation, commonly referred to as the flow equation:

$$\frac{d}{ds}\tilde{H}(s) = [\hat{\eta}(s), \tilde{H}(s)] \tag{4}$$

which allows $\tilde{H}(s)$ to be evaluated without explicitly constructing the full transformation $\hat{U}(s)$.

Introducing a flow parameter s, there exits a unitary transformation U_s, such that

$$\hat{H}_s = U_s^\dagger \hat{H} U_s \equiv \hat{H}_s^{\mathrm{d}} + \hat{H}_s^{\mathrm{od}}, \tag{5}$$

with the relations $U_{s=0} = \mathbf{1}$, and $\hat{H}_{s=0} = \hat{H}$. The transformation U_s is parametrized as

$$U_s = T_s \exp\left(\int_0^s ds' \hat{\eta}_{s'}\right),$$

where the anti-hermitian operator $\hat{\eta}_s$ serves as generator of the transformation. With T_s we denote s-ordering, which is defined equivalently to usual time-ordering. Taking the derivative of $\hat{H}_s$ with respect to s gives

$$\frac{d\hat{H}_s}{ds} = \frac{dU_s}{ds}\hat{H}U_s^\dagger + U_s\hat{H}\frac{dU_s^\dagger}{ds}. \tag{6}$$

Utilizing that for our particular form of U_s, we have that

$$\hat{\eta}_s = \frac{dU_s}{ds}U_s^\dagger = -U_s\frac{dU_s^\dagger}{ds} = -\hat{\eta}_s, \tag{7}$$

we obtain that

$$\frac{d\hat{H}_s}{ds} = \hat{\eta}_s\hat{H}_s - \hat{H}_s\hat{\eta}_s = \left[\hat{\eta}_s, \hat{H}_s\right]. \tag{8}$$

[2] Alternatively, this can also be reinterpreted as an s'-ordered integral. See [26, §6.1].

This is the key expression of the SRG method, describing the flow of the Hamiltonian. The specific unitary transformation is determined by the choice of $\hat{\eta}_s$. Through different choices of $\hat{\eta}_s$, the SRG evolution can be adapted to the features of a particular problem.

In-medium SRG One possibility to solve the flow equations is to choose a basis with respect to the physical vacuum state, set up the Hamiltonian matrix in this basis and solve Eq. (8) as a set of coupled first-order differential equations. However, since the size of the problem grows enormously with the number of particles and the size of the model space, the applicability of this free-space SRG method is restricted to comparatively small systems.

Instead of performing SRG in free space, the evolution can be done at finite density, i.e. directly in the A-body system [27]. This approach has recently been applied very successfully in nuclear physics [24, 28] and is called in-medium SRG (IM-SRG). The method allows the evolution of $3, ..., A$-body operators using only two-body machinery, with the simplifications arising from the use of normal-ordering with respect to a reference state.

In our case, we assume that the problem can be modelled by a Hamiltonian containing maximally two-body interactions. In second-quantized form, this one is given by

$$\hat{H} = \sum_{pq} \langle p| \hat{h}^{(0)} |q\rangle \, a_p^\dagger a_q + \frac{1}{4} \sum_{pqrs} \langle pq||rs\rangle \, a_p^\dagger a_q^\dagger a_s a_r, \quad (9)$$

where the operator $\hat{h}^{(0)}$ denotes the single-particle Hamiltonian, and the elements $\langle pq||rs\rangle$ are the anti-symmetrized two-body matrix elements. Normal-ordering with respect to a reference state $|\Phi_0\rangle$ yields

$$\hat{H} = E_0 + \sum_{pq} f_{pq} \{a_p^\dagger a_q\} + \frac{1}{4} \sum_{pqrs} v_{pqrs} \{a_p^\dagger a_q^\dagger a_s a_r\},$$

with Fock matrix elements

$$f_{pq} = \langle p| \hat{h}^{(0)} |q\rangle + \sum_i \langle pi||qi\rangle \,,$$

and where $v_{pqrs} = \langle pq||rs\rangle$ are the amplitudes of the two-body operator. Here and in the following, indices $i, j, k, ...$ denote hole states below the Fermi level, indices $a, b, c, ...$ particles states above the Fermi level, and indices $p, q, r, ...$ can be used for both particle and hole states. As reference state $|\Phi_0\rangle$ we choose the ground state of the non-interacting system, where all single-particle orbitals below the Fermi level are occupied.

Integrating the flow equations (8), we face one of the major challenges of the SRG method, namely the generation of higher and higher order interaction terms during the flow. With each evaluation of the commutator, the Hamiltonian gains terms of higher order, and these induced contributions will in subsequent integration steps contribute to terms of lower order. In principle, this continues to infinity.

To make the method computationally possible, we have to close the IM-SRG flow equations, suggesting that we are forced to truncate the equations to a certain order. We choose to truncate both $\hat{H}_s$ and $\hat{\eta}_s$ at the two-body level, an approach which is referred to as IM-SRG(2). This normal-ordered two-body approximation seems to be sufficient in many cases and has yielded excellent results for several nuclei [24, 28, 29].

The commutator in the flow equations (8) guarantees that the IM-SRG wave function $U_s^\dagger |\Phi\rangle$ can be expanded in terms of linked diagrams only [30, 31], which suggests that IM-SRG is size-extensive. Regarding the quality of the SRG results, it means that the error introduced by truncating the many-body expansions scales linearly with the number of particles N.

With this truncation, the generator $\hat{\eta}$ can be written as

$$\hat{\eta} = \sum_{pq} \eta_{pq}^{(1)} \{a_p^\dagger a_q\} + \frac{1}{4} \sum_{pqrs} \eta_{pqrs}^{(2)} \{a_p^\dagger a_q^\dagger a_s a_r\},$$

where $\eta_{pq}^{(1)}$ and $\eta_{pqrs}^{(2)}$ are the one- and two-body elements, respectively. Making use of the permutation operator $\hat{P}_{pq} f(p,q) = f(q,p)$, the IM-SRG(2) flow equations are given by

$$\frac{dE_0}{ds} = \sum_{ia} \left(\eta_{ia}^{(1)} f_{ai} - \eta_{ai}^{(1)} f_{ia} \right) + \frac{1}{2} \sum_{ijab} \eta_{ijab}^{(2)} v_{abij}, \quad (10)$$

$$\frac{df_{pq}}{ds} = \sum_{r} \left(\eta_{pr}^{(1)} f_{rq} + \eta_{qr}^{(1)} f_{rp} \right) + \sum_{ia} \left(1 - \hat{P}_{ia} \right) \left(\eta_{ia}^{(1)} v_{apiq} - f_{ia} \eta_{apiq}^{(2)} \right)$$
$$+ \frac{1}{2} \sum_{aij} \left(1 + \hat{P}_{pq} \right) \eta_{apij}^{(2)} v_{ijaq} + \frac{1}{2} \sum_{abi} \left(1 + \hat{P}_{pq} \right) \eta_{ipab}^{(2)} v_{abiq}, \quad (11)$$

$$\frac{dv_{pqrs}}{ds} = \sum_t \left(1-\hat{P}_{pq}\right)\left(\eta^{(1)}_{pt} v_{tqrs} - f_{pt}\eta^{(2)}_{tqrs}\right) - \sum_t \left(1-\hat{P}_{rs}\right)\left(\eta^{(1)}_{tr} v_{pqts} - f_{tr}\eta^{(2)}_{pqts}\right)$$
$$+ \frac{1}{2}\sum_{ab}\left(\eta^{(2)}_{pqab} v_{abrs} - v_{pqab}\eta^{(2)}_{abrs}\right) - \frac{1}{2}\sum_{ij}\left(\eta^{(2)}_{pqij} v_{ijrs} - v_{pqij}\eta^{(2)}_{ijrs}\right)$$
$$- \sum_{ia}\left(1-\hat{P}_{ia}\right)\left(1-\hat{P}_{pq}\right)\left(1-\hat{P}_{rs}\right)\eta^{(2)}_{aqis} v_{ipar}. \tag{12}$$

Note that for brevity, we skip all s-dependence in the equations.

Choice of generator

To determine the specific unitary transformation, one needs to specify the generator $\hat{\eta}$. Through different choices, the SRG flow can be adapted to the features of a particular problem.

Wegner's canonical generator The original choice, suggested by Wegner [32], reads

$$\hat{\eta} = \left[\hat{H}^{\mathrm{d}}, \hat{H}^{\mathrm{od}}\right] = \left[\hat{H}^{\mathrm{d}}, \hat{H}\right]. \tag{13}$$

As commutator between two Hermitian operators, $\hat{\eta}$ fulfils the criterion of antihermiticity and can be shown to suppress the off-diagonal matrix elements [27]. In general, matrix elements far off the diagonal, where the Hamiltonian connects states with large energy differences, are suppressed much faster than elements closer to the diagonal.
Evaluating the commutator, we get for the one- and two-body elements

$$\eta^{(1)}_{pq} = \sum_r \left(f^d_{pr} f_{rq} - f_{pr} f^d_{rq}\right) + f_{pq} v^d_{qppq}\left(n_q - n_p\right)$$
$$\eta^{(2)}_{pqrs} = -\sum_t \left\{\left(1-\hat{P}_{pq}\right) f_{pt} v^d_{tqrs} - \left(1-\hat{P}_{rs}\right) f_{tr} v^d_{pqts}\right\}$$
$$+ \sum_t \left\{\left(1-\hat{P}_{pq}\right) f^d_{pt} v_{tqrs} - \left(1-\hat{P}_{rs}\right) f^d_{tr} v_{pqts}\right\}$$
$$+ \frac{1}{2}\sum_{tu}(1-n_t-n_u)\left(v^d_{pqtu} v_{turs} - v_{pqtu} v^d_{turs}\right)$$
$$+ \sum_{tu}(n_t - n_u)\left(1-\hat{P}_{pq}\right)\left(1-\hat{P}_{rs}\right) v^d_{tpur} v_{uqts},$$

where we use the standard notation

$$n_p = \begin{cases} 1, & \text{if } p < \epsilon_F \quad (p \text{ is hole state}) \\ 0, & \text{if } p > \epsilon_F \quad (p \text{ is particle state}) \end{cases}.$$

White's generator Apart from this canonical generator, there exist several other ones in literature. One of them is White's choice [33], which makes numerical approaches much more efficient. The problem with Wegner's generator are the widely varying decaying speeds of the elements, removing first terms with large energy differences and then subsequently those ones with smaller energy separations. That way the flow equations become a stiff set of coupled differential equations, which often gets numerically unstable.
White takes an alternative approach, which is especially suited for problems where one is interested in the ground state of a system. Instead of driving all off-diagonal elements of the Hamiltonian to zero, he focuses solely on those ones that are connected to the reference state $|\Phi_0\rangle$, aiming to decouple the reference state from the remaining Hamiltonian. With a suitable transformation, the elements get similar decaying speeds, which solves the problem of stiffness of the flow equations. The generator is explicitly constructed the following way [28, 33]

$$\hat{\eta} = \sum_{ai} \frac{f_{ai}}{f_a - f_i - v_{aiai}}\{a^\dagger_a a_i\} - \mathrm{hc}$$
$$+ \sum_{abij} \frac{v_{abij}}{f_a + f_b - f_i - f_j + A_{abij}}\{a^\dagger_a a^\dagger_b a_j a_i\} - \mathrm{hc}, \tag{14}$$

with $f_p \equiv f_{pp}$, 'hc' denoting the Hermitian conjugate, and

$$A_{abij} = v_{abab} + v_{ijij} - v_{aiai} - v_{ajaj} - v_{bibi} - v_{bjbj}.$$

Compared to Wegner's canonical generator, where the final flow equations involve third order powers of the f- and v-elements, these elements contribute only linearly with White's generator, which results in much better numerical properties.

We may attempt follow the same technique as for Hartree-Fock and reduce the operator problem into a linear algebra problem by evaluating the operator using a single-particle basis. However, since a commutator between two-body operators can result in a three-body operator, it follows that as s increases, the evolved Hamiltonian $\tilde{H}(s)$ can gain terms that couple more and more particles. It is not practical to keep all such terms, especially since higher-body operators are much more computationally expensive.

In-medium SRG follows the same procedure as with ordinary SRG, but the calculations are performed relative to some reference state rather than the vacuum state. This is advantageous for systems with many-particles as the effect of truncation is not quite as drastic as it would be in SRG [[true/false?]].

[[need some more content before diving straight into the algebra]]

Normal-ordering is a syntactic operation that reorders a product of operators so as to eliminate all but the highest-body interaction. The operation is must be defined against a fixed many-body state, such as the vacuum state. We denote normal ordering using $:\ldots:$, with with the state given by context.

Normal-ordering with respect to the vacuum state is performed by rearranging the operator product such that every $\hat{a}^\dagger$ appear before $\hat{a}$, with the caveat that the parity of the permutation must also be applied to the sign of the result.

For many-body problems involving large number of particles, the vacuum state is not very convenient as it requires the application of many creation operators to reach the states of interest. Therefore, it is preferable to utilize some reference state Φ (a Slater determinant) so that any other state can be readily expressed as some excitation from this state.

Given a reference state Φ, we may define a set of *quasi-particle creation and annihilation operators* $\hat{b}^\dagger$ and $\hat{b}$ that obey the same commutation relations as the $\hat{a}$ operators. The two sets of operators are related by:

$$\hat{b}_p^\dagger \equiv \begin{cases} \hat{a}_p^\dagger & \text{if } p \text{ is unoccupied in } \Phi \\ \hat{a}_p & \text{if } p \text{ is occupied in } \Phi \end{cases}$$

Analogously, there is a similar notion of normal-ordering with respect to the reference state: namely, the rearrangement operators such that every $\hat{b}^\dagger$ appears before $\hat{b}$.

The relationship between the $\hat{b}$ operators and Φ is completely analogous to the relationship between the $\hat{a}$ operators and 0. As a result, theorems governing these operators can be applied to both. In particular, *Wick's theorem* – an algebraic theorem that allows complicated strings of creation and annihilation operators to be simplified algorithmically – plays an important role in simplifying the equations of IM-SRG.

For conciseness, we introduce the notation $\hat{A}^\dagger_{q_1,\ldots,q_k}$ to denote the normal-ordered string of creation operators $\hat{a}^\dagger_{p_1}\ldots\hat{a}^\dagger_{p_k}$, and similarly for $\hat{B}^\dagger$ as well as their annihilation counterparts. Note that this implies that the ordering is reversed in the annihilation version of this notation.

[[...]]

For our purposes, we restrict ourselves to at most two-body operators, and thus any higher-body operators that emerge from the commutator are neglected. In this approximation, the method is known as "IMSRG (2)". The loss of three-body and higher terms one of the two sources of error in this method, the other being the basis truncation.

The heart of the method lies in the choice of the generator $\eta(s)$. We would like to choose the generator such that as $s \to \infty$ the transformed Hamiltonian $\tilde{H}(s)$ approaches either a diagonal, block-diagonal, or band-diagonal form, all of which reduce the amount of effort needed to solve the problem. For our problem, we choose to decouple the ground state from all the excited states in the Hamiltonian matrix using a carefully chosen generator. Doing so allows us to readily recover the ground state energy.

There are two commonly used generators: the Wegner generator and the White generator. The Wegner generator has been known since the introduction of the SRG method by Wegner[32] and has a particularly simple form:

$$\hat{\eta}^{\mathrm{g}}(s) \equiv [\hat{H}^{\mathrm{d}}(s), \hat{H}(s)]$$

where $\hat{H}^{\mathrm{d}}$ denotes the diagonal component of $\hat{H}$. Despite its apparently simplicity, it does not work particularly well in practice as the off-diagonal elements vanish at vastly different rates, leading to differential equations that are typically stiff.

The White generator remedies this problem by introducing denominators for each term to control and normalize the rate at which off-diagonal elements vanish:

$$\hat{\eta}^{\mathrm{h}}(s) \equiv \sum_{\substack{a \\ p_1,\ldots,p_a \\ q_1,\ldots,q_a}} \frac{\langle\Phi_{p_1,\ldots,p_a}|\hat{H}^{[a]}|\Phi_{q_1,\ldots,q_a}\rangle \hat{B}^\dagger_{p_1,\ldots,p_a}\hat{B}_{q_1,\ldots,q_a}}{E_{p_1,\ldots,p_a} - E_{q_1,\ldots,q_a}}$$

where [[note: haven't explained what $\hat{b}$ means]]

$$E_{p_1,\ldots,p_a} \equiv \langle\Phi_{p_1,\ldots,p_a}|\hat{H}|\Phi_{p_1,\ldots,p_a}\rangle$$
$$\hat{B}^\dagger_{p_1,\ldots,p_a} \equiv \hat{b}^\dagger_{p_1}\cdots\hat{b}^\dagger_{p_a}$$

and $\hat{H}^{[a]}$ denotes the a-body term of the Hamiltonian. As a result of this modification, the White generator exhibits better numerical stability and is computationally less expensive than the Wegner generator.

An accurate and robust ODE solver is required to solve (4). In particular, the solver must be able to handle the stiffness that can often arise (even in the case of White generator). For this, we use an accurate, high-order ODE solver implementation by Shampine and Gordon that uses the Adams predictor-corrector formulas [[Ref: Shampine and Gordon book]].

[[...]]

Expanding the commutator leads to the expression

$$[\hat{\eta}, \hat{H}] = \hat{C}(\hat{\eta}, \hat{H}) - \hat{C}(\hat{H}, \hat{\eta})$$

where $\hat{C}$ is defined diagrammatically in Figure 2. For IM-SRG(2), we truncate the commutator to a two-body operator, neglecting the three-body term.

D. The self-energy correction

IM-SRG, in the form described, does not provide a means to obtain ground state energies of open-shell systems. While there exists a multi-reference IM-SRG that can handle the general problem ([[cite Heiko?]]), we opted to use a much simpler approach to obtain the addition

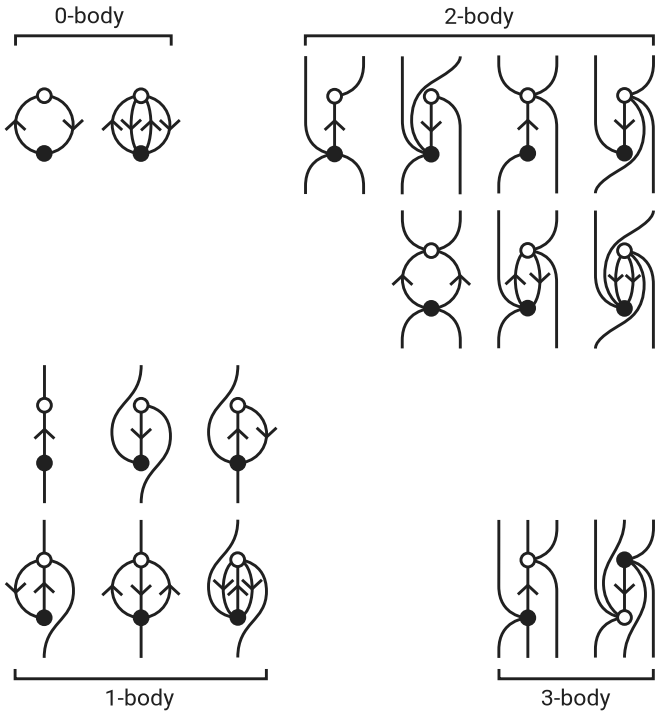

FIG. 2. Diagrammatic form of $\hat{C}(\circ, \bullet)$.

and removal energies: quasidegenerate perturbation theory (QDPT). In QDPT, the solutions of the approximate Hamiltonian $\hat{H}^{\mathrm{o}}$ are used as the basis of the model space. One then assumes the existence of an operator $\hat{\Omega}$, known as the *wave operator*, that maps some set of states $\tilde{\Phi}_u$ within the model space to the exact ground state Ψ_u:

$$\Psi_u = \hat{\Omega}\tilde{\Phi}_u \tag{15}$$

The states $\tilde{\Phi}_u$ consist of some mixture of the eigenstates $\Phi_{u'}$ of the approximate Hamiltonian $\hat{H}^{\mathrm{o}}$.

There is some freedom in the choice of the wave operator $\hat{\Omega}$. We assume it has the following form:

$$\hat{\Omega} = \hat{P} + \hat{Q}\hat{\Omega}\hat{P} \tag{16}$$

where $\hat{P}$ projects any state into the model space and $\hat{Q}$ is the complement of $\hat{P}$. This entails that the exact states Ψ_u is no longer normalized but instead satisfies the typical intermediate normalization: $\langle\Psi_u|\tilde{\Phi}_u\rangle = 1$.

Making use of the assumptions in Eq. (15) and (16), one can derive from the Schrödinger equation the generalized Bloch equation, the main equation of QDPT:

$$[\hat{\Omega}, \hat{H}^{\mathrm{o}}] = (1 - \hat{\Omega})\hat{V}\Omega$$

where $\hat{V} \equiv \hat{H} - \hat{H}^{\mathrm{o}}$ is the perturbation. The commutator on the left may be "inverted" using the resolvent approach [[ShavittBartlett,p.50]], resulting in:

$$\hat{Q}\Omega\hat{P}_u = \hat{R}_u(1 - \hat{\Omega})\hat{V}\Omega\hat{P}_u$$

where $\hat{R}_u \equiv \hat{Q}(E_u - \hat{Q}\hat{H}^{\mathrm{o}}\hat{Q})^{-1}\hat{Q}$ is the resolvent and $\hat{P}_u$ projects any state onto Φ_u. As is typical in perturbation theory, we assume $\hat{\Omega}$ can be expanded as a series of the increasing order as measured by the "power" of the perturbation $\hat{V}$:

$$\hat{\Omega} = \hat{P} + \hat{Q}\big(\hat{\Omega}_1 + \hat{\Omega}_2 + \cdots\big)\hat{P}$$

This leads to a recursion relation of $\hat{\Omega}$ that enables $\hat{\Omega}$ to be calculated up to any order, as least in theory. Here, we show $\hat{\Omega}$ up to third order: [[double-check]]

$$\begin{aligned}
\hat{\Omega}_1\hat{P}_u &= \hat{R}_u\hat{V}\hat{P}_u \\
\hat{\Omega}_2\hat{P}_u &= \hat{R}_u\Big(\hat{V}\hat{R}_u - \sum_v \hat{R}_v\hat{V}\hat{P}_v\Big)\hat{V}\hat{P}_u \\
\hat{\Omega}_3\hat{P}_u &= \hat{R}_u\Big(\hat{V}\hat{R}_u\hat{V}\hat{R}_u - \hat{V}\hat{R}_u\sum_v \hat{R}_v\hat{V}\hat{P}_v \\
&\qquad - \sum_v \hat{R}_v\hat{V}\hat{P}_v\hat{V}\hat{R}_u - \sum_v \hat{R}_v\hat{V}\hat{R}_v\hat{V}\hat{P}_v \\
&\qquad + \sum_v \hat{R}_v\sum_w \hat{R}_w\hat{V}\hat{P}_w\hat{V}\hat{P}_v\Big)\hat{V}\hat{P}_u
\end{aligned}$$

[[Since the systems are all closed-shell, the diagonal approximation can be used here to simplify the calculations.]]

[[Discuss how]] The diagrams for each order of correction can be evaluated using algebraic or diagrammatic techniques. The second-order correction is given by

$$\epsilon_p = \frac{1}{2}\Bigg(\sum_{iab}\frac{|V_{piab}|^2}{f_p + f_i - f_a - f_b} - \sum_{ija}\frac{|V_{ijpa}|^2}{f_i + f_j - f_p - f_a}\Bigg)$$

and depicted in Figure 3. Since there are numerous terms in the third-order correction, they are simply listed in a diagrammatic form in Figure 3.

[[...]]

E. Diffusion Monte Carlo

Diffusion Monte Carlo (DMC) is a method for calculating the ground state properties via a stochastic process akin to classical diffusion, refining an approximate ground state density towards that of the exact ground state. The rules that govern the diffusion process are obtained by evolving the wave function using what can be formally be thought of as the time-dependent Schrödinger equation along imaginary time $t = \mathrm{i}\tau$:

$$\frac{\partial}{\partial\tau}|\Phi(\tau)\rangle = \hat{H}|\Phi(\tau)\rangle \tag{17}$$

The solutions to this equation are not unlike the ordinary Schrödinger equation with a slight but crucial difference in the exponent:

$$|\Phi(\tau)\rangle = \mathrm{e}^{-\hat{H}\tau}|\Phi(0)\rangle$$

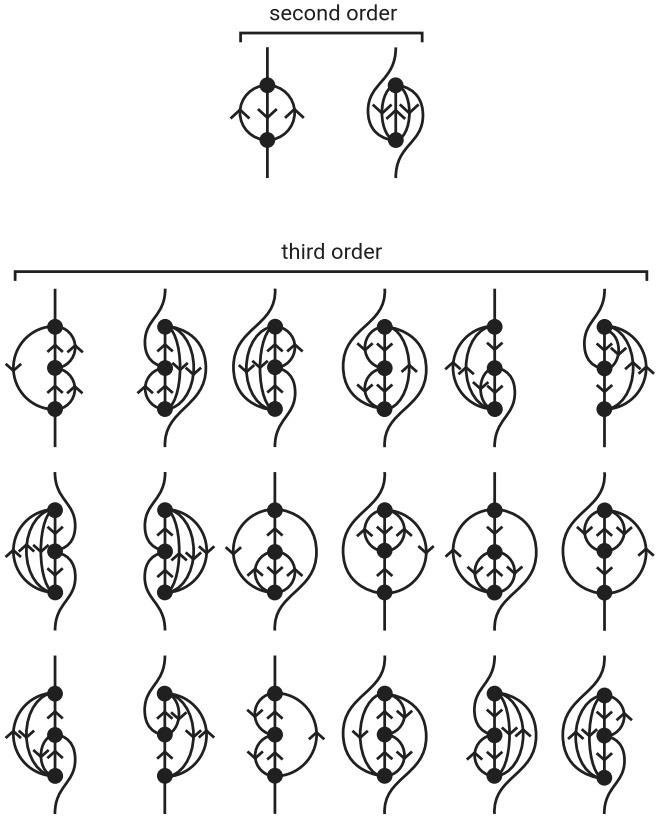

FIG. 3. Diagrammatic form of the second- and third-order self-energy corrections.

where $|\Phi(0)\rangle$ is the initial wave function at $\tau = 0$ – not to be confused with the exact ground state of $\hat{H}$, which we denote $|\Psi_0\rangle$ here. If we decompose the wave function into a sum over the eigenstates $|\Psi_n\rangle$,

$$|\Psi(\tau)\rangle = \mathrm{e}^{-\hat{H}\tau} \sum_n c_n |\Psi_n\rangle = \sum_n c_n \mathrm{e}^{-E_n\tau} |\Psi_n\rangle$$

we find that components of the wave function that have negative energy will increase exponentially as $\tau \to \infty$, while those with positive energy will decrease exponentially. This property can be exploited to filter out the undesirable components, leaving only the ground state energy. To do this, we require a trial energy E_T – a guess of the ground state energy – and replace $\hat{H}$ in (17) with $(\hat{H} - E_\mathrm{T})$ so that, if our trial energy is good, all states but the ground states will approximately vanish.

Diffusion Monte-Carlo (DMC) is a method used for refining a crude estimate to the ground state density into a better approximation to the exact ground state. The basic idea is to move multiple random walkers in position space with sampling rules which ensures convergence to a behavior representing a walk guided by the exact ground state density. Once a satisfying level of convergence is reached, expectation values are calculated by accumulating local estimates along the path of the walkers.

The equations representing the DMC algorithm is obtained by applying the projection operator $\hat{P}(\tau)$ on the crude trial state $|\Psi_T\rangle$

$$\hat{P}(\tau)\,|\Psi_T\rangle \equiv \exp\Big(-(\hat{H} - E_0)\tau\Big)\,|\Psi_T\rangle \tag{18}$$

where τ is a constant often described as imaginary time, and $E_0 = \langle\Psi_0|\,\hat{H}\,|\Psi_0\rangle$ is the ground state of the Hamiltonian $\hat{H}$. By expanding the trial state in the eigenfunctions of $\hat{H}$, the ground state is obtained up to a constant factor

$$\lim_{\tau\to\infty} \langle\mathbf{r}|\,\hat{P}(\tau)\,|\Psi_T\rangle = \langle\Psi_0|\Psi_T\rangle\,\Psi_0(\mathbf{r}). \tag{19}$$

Defining $\Phi(\mathbf{r},\tau) \equiv \langle\mathbf{r}|\,\hat{P}(\tau)\,|\Psi_T\rangle$, we obtain the state at a later time $\tau + \delta\tau$ through projection

$$\begin{aligned}
\Phi(\mathbf{r},\tau+\delta\tau) &= \langle\mathbf{r}|\,P(\tau+\delta\tau)\,|\Psi_T\rangle \\
&= \langle\mathbf{r}|\exp\Big(-(\hat{H}-E_0)\delta\tau\Big)\,\hat{P}(\tau)\,|\Psi_T\rangle \\
&= \langle\mathbf{r}|\exp\Big(-(\hat{H}-E_0)\delta\tau\Big)\,|\Phi(\tau)\rangle \\
&= \int \mathrm{d}\mathbf{r}'\,\langle\mathbf{r}|\exp\Big(-(\hat{H}-E_0)\delta\tau\Big)\,|\mathbf{r}'\rangle\,\Phi(\mathbf{r}',\tau) \\
&\equiv \int \mathrm{d}\mathbf{r}' G(\mathbf{r},\mathbf{r}';\delta\tau)\Phi(\mathbf{r}',\tau).
\end{aligned} \tag{20}$$

In practice, the ground state energy is a priori unknown, hence a trailing averaged value obtained from the converging DMC density is used. This energy is often referred to as the trial energy, and it is believed that with a sufficiently good trial state, the error due to this approximation is small.

The Green's function introduced in Eq. (20) has singularities due to the the Coulomb interaction term in $\hat{H}$. Due to Pauli exclusion these are not physical, nevertheless, in numerical implementations they are unpredictable and undesirable, hence we want to avoid them.

For evaluation of the local energy, the trial state is designed to cancel the Coulomb singularities by containing so-called correlation factors, however, this cancellation does not apply to the terms in the Green's function. In order to transfer this behavior to apply to the Green's function, a change to the formalism is introduced by iterating on a mixed density $f(\mathbf{r},\tau) \equiv \Phi(\mathbf{r},\tau)\Psi_T(\mathbf{r})$. Note that all previous arguments regarding convergence to the true ground state still applies for the new distribution.

Methods exist for transforming the mixed density into the pure density $|\Phi(\mathbf{r},\tau)|^2$ [34], but unless the pure density is explicitly needed (e.g. for comparisons with other methods), this is strictly not necessary.

Additionally, to avoid issues regarding the positive definiteness of the mixed distribution, the nodes of the mixed density is fixed to those of the wave function of the trial state. This is known as the *fixed node approximation* [34, 35]. Again, given a sufficiently good trial state, the errors should be small.

The Green's function for the mixed density is given as [35]

$$G(\mathbf{r},\mathbf{r}';\delta\tau)_f = \langle \mathbf{r}| \exp\left(\frac{1}{2}\nabla\cdot[(\nabla-\mathbf{F}(\mathbf{r}))] - (E_L(\mathbf{r})-E_T)\right)|\mathbf{r}'\rangle \tag{21}$$

$$\propto e^{-\left[|\mathbf{r}-\mathbf{r}'-\frac{1}{2}\delta\tau\mathbf{F}(\mathbf{r})|^2/2\delta\tau\right]} \tag{22}$$

$$\times\, e^{-\left[\frac{1}{2}\left[E_L(\mathbf{r}')+E_L(\mathbf{r})\right]-E_T\right]\delta\tau} + \mathcal{O}(\delta\tau^2),$$

where

$$\mathbf{F}(\mathbf{r}) = 2\Psi_T(\mathbf{r})^{-1}\nabla\Psi_T(\mathbf{r}) \tag{23}$$

is the drift vector commonly referred to as the *quantum force*.

The local energy

$$E_L(\mathbf{r}) = \Psi_T(\mathbf{r})^{-1}\hat{H}\Psi_T(\mathbf{r}) \tag{24}$$

is necessarily sampled from $|\Psi_T(\mathbf{r})|^2$ (ensured by using the Metropolis Algorithm [34]) to avoid undefined energies when sampling close to the nodes of $\Psi_T(\mathbf{r})$.

The Green's function from Eq. (**??**) has been split into two for practical reasons; one part containing the kinetic terms, more specifically this represents a Fokker-Planck diffusion process, and a second part which is commonly referred to as a *branching function*, which is an effective reweighing of a positions contribution to the overall density. Excluding branching we will simply sample from the density of the trial state.

In order dampen the errors introduced by splitting the Green's function, the time step $\delta\tau$ should be small. A value in the range of 10^{-3} to 10^{-4} is used in this work. High variance in energy samples requires a smaller time step to keep the branching controlled, since the fluctuations of the two are connected by Eq. (22).

The name branching arise from the fact that in DMC, the weights are implemented as a probability of a given walker to copy or delete itself n times, where $\langle n\rangle$ equals the branching term of Eq. (22). Let G_b denote the value of the branching function at a given position. Correct weighting is then ensured by guaranteeing $m = \max(\text{floor}(G_b)-1, 0)$ branches with a probability $G_b - m$ of getting an additional branch. A branch is an identical copy of the corresponding walker, with an identical past but with a different future. When the number of requested branches is zero, the walker is removed from the simulation.

Initially, N_w walkers are initialized to span $|\Psi_T(\mathbf{r})|^2$. This is ensured by using the Metropolis Algorithm. Moreover, importance sampling is ensured by sampling according to the kinetic term of Eq. (21) *cite solution langevin*

$$x_{i+1} = x_i + \frac{1}{2}\delta\tau F(\mathbf{r})_x + \xi, \tag{25}$$

where ξ is a uniform distributed random number with variance $\text{Var}(\xi) = 2D\delta\tau$. A typical value of N_w in this work is 250 000.

For each time step, diffusion and branching repeats a given number of blocks N_b for each walker. New branches are not active until the next time step, and if a walker hits zero branches the block repetition stops. During these block loops, the trial energy E_T is sampled for use in the next time step $k+1$

$$E_T^{k+1} = \frac{1}{M^{(k)}}\sum_{i=1}^{M^{(k)}} G_b(\mathbf{r}_i^{(k)})E_L(\mathbf{r}_i^{(k)}), \tag{26}$$

where $M^{(k)}$ is the total number of samples obtained in cycle k. For this work we have found a value of $N_b = 100$ to be sufficient.

Several methods for estimating E_0 exist in the literature, one of which is simply an average of all N_c trial energies calculated after N_t thermalization cycles

$$E_0 = \frac{1}{N_c - N_t}\sum_{k=N_t}^{N_c} E_T^{(k)}. \tag{27}$$

This is the relation we use in this work to obtain the DMC energies.

In this work, the trial state has been chosen to consist of a single Slater determinant (cite) together with a single variational parameter Pad-Jastrow correlation function (cite).

The Slater determinant contains eigenstates $\phi_n(\mathbf{r})$ of Eq. (**??**) with a variational parameter α scaling the oscillator frequency ω such that $\omega \to \alpha\omega$ in all solutions:

$$\phi_n(\mathbf{r}) = H_n(\sqrt{\alpha\omega}x)H_n(\sqrt{\alpha\omega}y)\exp(-\alpha\omega r^2), \tag{28}$$

where H_n is the n'th level Hermite polynomial.

The eigenstates are selected such that the N lowest lying energy eigenstates are selected (counting spin-degeneracy). Due to the Hamiltonian being spin independent we may split the Slater determinant into two equal parts - one for each spin level (cite). The overall form of the trial state is as follows:

$$\Psi_T(\mathbf{r}) = S(\mathbf{r}^\uparrow)S(\mathbf{r}^\downarrow)\prod_{i<j}^{N} J(r_{ij}), \tag{29}$$

with

$$S(\mathbf{r}^s) = \begin{vmatrix} \phi_1(\mathbf{r}_1^s) & \phi_2(\mathbf{r}_1^s) & \cdots & \phi_{\frac{N}{2}}(\mathbf{r}_1^s) \\ \phi_1(\mathbf{r}_2^s) & \phi_2(\mathbf{r}_2^s) & \cdots & \phi_{\frac{N}{2}}(\mathbf{r}_2^s) \\ \vdots & \vdots & \ddots & \vdots \\ \phi_1(\mathbf{r}_{\frac{N}{2}}^s) & \phi_2(\mathbf{r}_{\frac{N}{2}}^s) & \cdots & \phi_{\frac{N}{2}}(\mathbf{r}_{\frac{N}{2}}^s) \end{vmatrix}, \tag{30}$$

and

$$J(r_{ij}) = \exp\left(\frac{r_{ij}}{1+\beta r_{ij}}\right), \tag{31}$$

where $\mathbf{r}_i^s$ denotes i'th particle with spin s, and r_{ij} is the relative distance between two electrons. Since Metropolis Monte-Carlo only involves ratios of density functions, all normalization factors are skipped.

As a consequence of the variational principle, the optimal numeric values for α and β can be found by minimizing the energy in the variational parameter space. For this we have used the adaptive step gradient descent method (cite ASGD).

Using a single Slater determinant and a single variational parameter in the correlation function might at first glance seem insufficient, however, the strength and robustness of DMC greatly succeeds at transforming this naive approximation into a very good estimate to the ground state density. It should be mentioned that for systems where the single-particle Hamiltonian does not have analytical solutions, this approach will indeed be insufficient due to low overlap between the initial and exact state.

A single Slater determinant and a simple correlation function opens up numerous optimization schemes which trivializes the CPU-time of most calculations. We refer to Refs (cite optimization techniques) for more information. Moreover, the most costly part of evaluating the single-particle eigenstates, the exponentials, is independent of the quantum number n, and can thus be tabulated once for the entire calculation. This holds for the gradient and Laplacian needed in the quantum force and local energy, respectively, since the exponential shape is preserved under differentiation.

III. RESULTS

In Figure **??** we show the calculated ground state energies from Hartree-Fock, second-order (Møller-Plesset) perturbation theory (MPPT), and IMSRG. The exact result from diffusion Monte Carlo (DMC) is also shown as a dashed line in systems where it is known [13].

Both perturbation theory and IMSRG add corrections in addition to the Hartree-Fock results to recover the correlation energy and they do quite well in recovering the correlation energy in the system. Compared with MPPT, IMSRG generally converges faster, although does not always converge to the DMC result. Generally speaking, IMSRG is closer to the DMC result as the number of particles increases.

There are a few cases where the IMSRG over-corrects the result, leading to a ground state energy that is lower than the exact result. This is not unexpected given that, unlike Hartree-Fock, IMSRG is non-variational. These tend to occur when the number of particles is few, or the frequency is very low (high correlation). However,

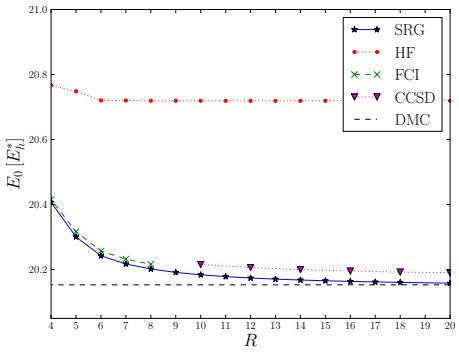

(a)Results for $N = 6$ and $\omega = 1.0$

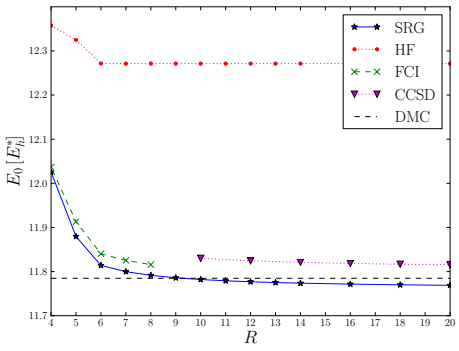

(b)Results for $N = 6$ and $\omega = 0.5$

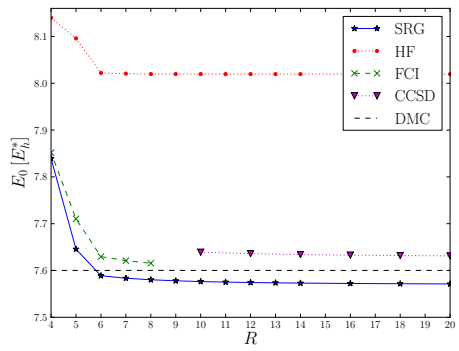

(c)Results for $N = 6$ and $\omega = 0.28$

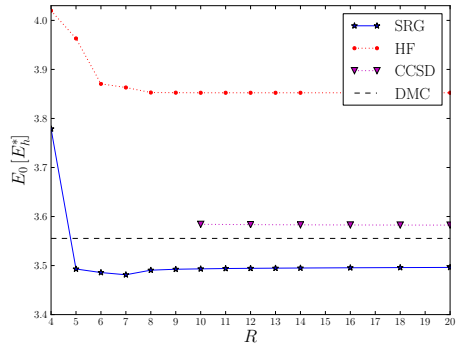

(d)Results for $N = 6$ and $\omega = 0.1$

FIG. 4. Comparison of our IM-SRG(2) ground state energies (SRG) for circular quantum dots for $N = 6$ and $\omega = 1.0$ The results are compared with diffusion Monte Carlo (DMC), coupled cluster at the level of singles and doubles (CCSD), full configuration interaction (FCI) and Hartree-Fock calculations (HF) as functions of the number of major oscillator shells

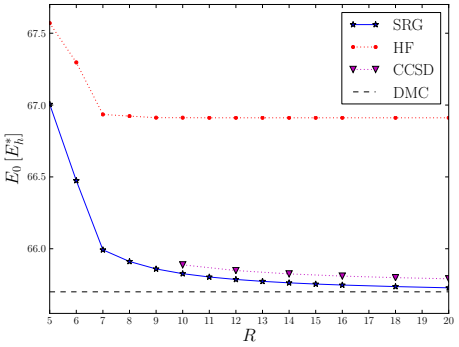

(a)Results for $N = 12$ and $\omega = 1.0$

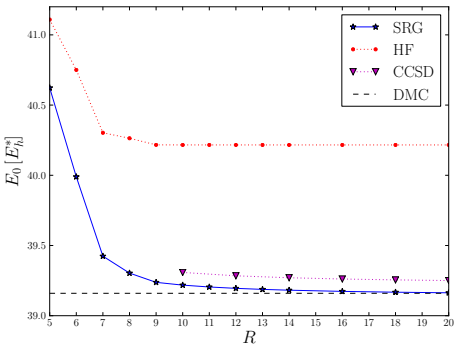

(b)Results for $N = 12$ and $\omega = 0.5$

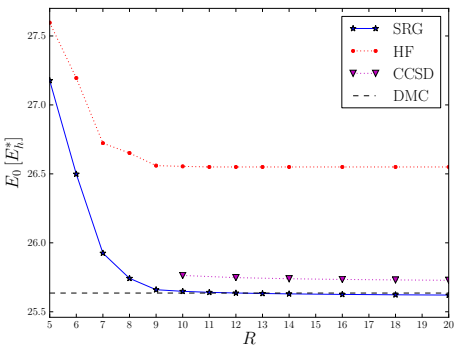

(c)Results for $N = 12$ and $\omega = 0.28$

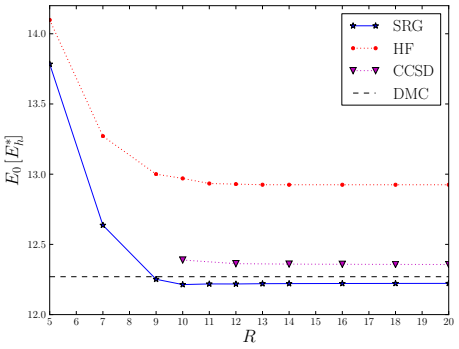

(d)Results for $N = 12$ and $\omega = 0.1$

FIG. 5. Comparison of our IM-SRG(2) ground state energies (SRG) for circular quantum dots for $N = 12$ and different values of ω. The results are compared with diffusion Monte Carlo (DMC), coupled cluster at the level of singles and doubles (CCSD), full configuration interaction (FCI) and Hartree-Fock calculations (HF) as functions of the number

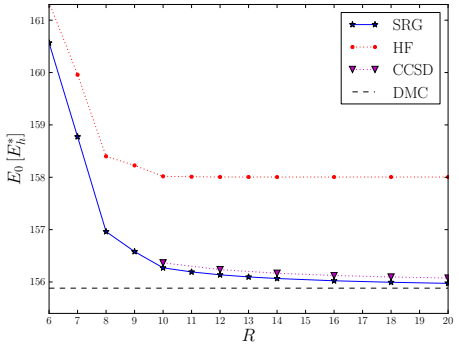

(a)Results for $N = 20$ and $\omega = 1.0$

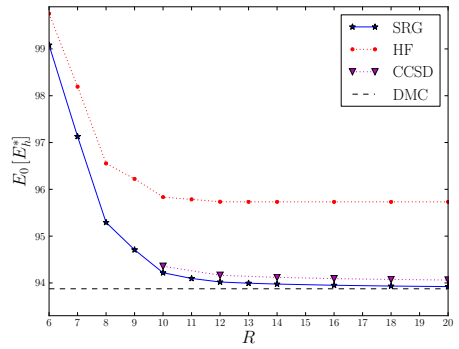

(b)Results for $N = 20$ and $\omega = 0.5$

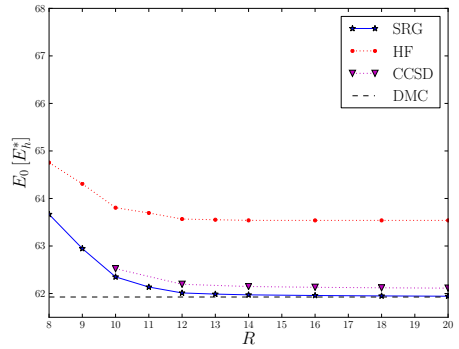

(c)Results for $N = 20$ and $\omega = 0.28$

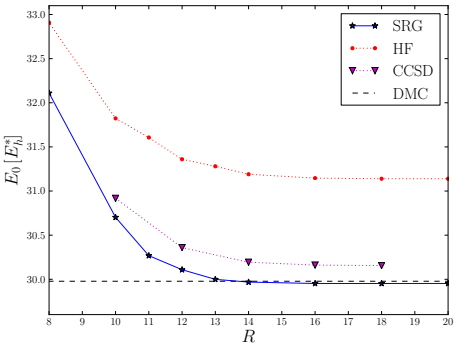

(d)Results for $N = 20$ and $\omega = 0.1$

FIG. 6. Comparison of our IM-SRG(2) ground state energies (SRG) for circular quantum dots for $N = 20$ and different values of ω. The results are compared with diffusion Monte Carlo (DMC), coupled cluster at the level of singles and doubles (CCSD), full configuration interaction (FCI) and Hartree-Fock calculations (HF) as functions of the number

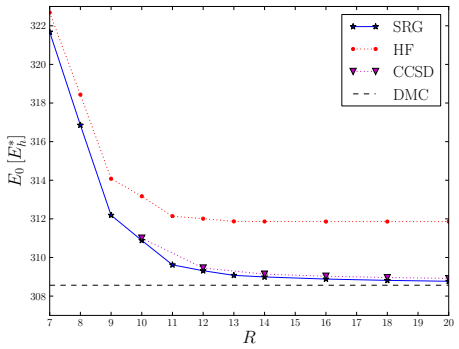

(a)Results for $N = 30$ and $\omega = 1.0$

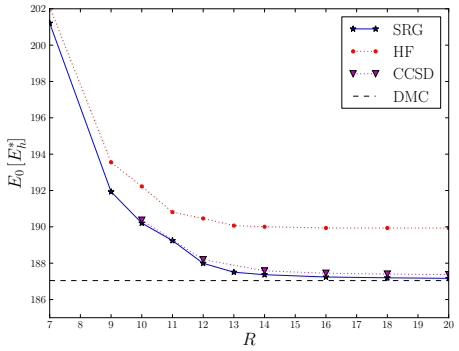

(b)Results for $N = 30$ and $\omega = 0.5$

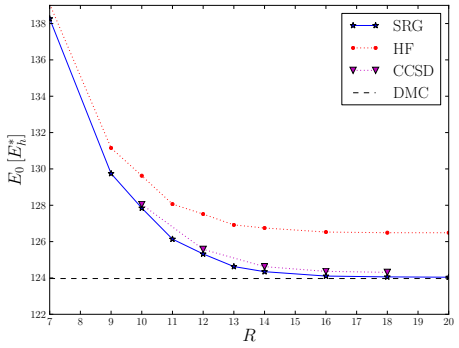

(c)Results for $N = 30$ and $\omega = 0.28$

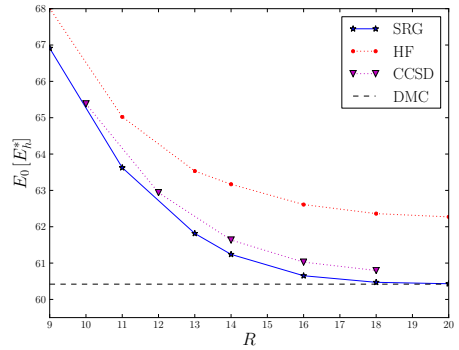

(d)Results for $N = 30$ and $\omega = 0.1$

FIG. 7. Comparison of our IM-SRG(2) ground state energies (SRG) for circular quantum dots for $N = 30$ and different values of ω. The results are compared with diffusion Monte Carlo (DMC), coupled cluster at the level of singles and doubles (CCSD), full configuration interaction (FCI) and Hartree-Fock calculations (HF) as functions of the number

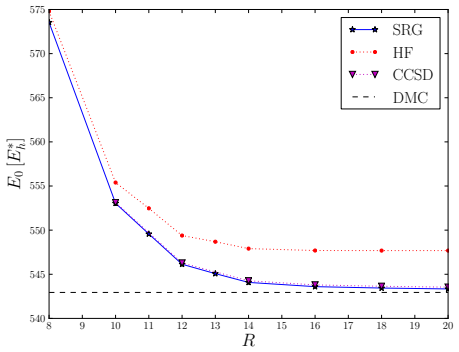

(a)Results for $N = 42$ and $\omega = 1.0$

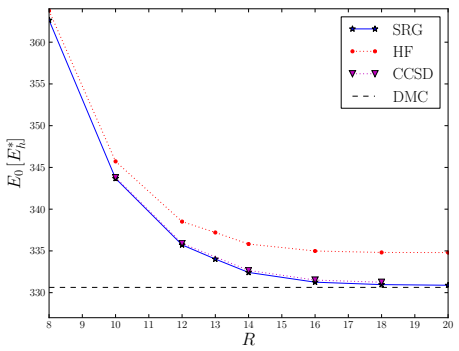

(b)Results for $N = 42$ and $\omega = 0.5$

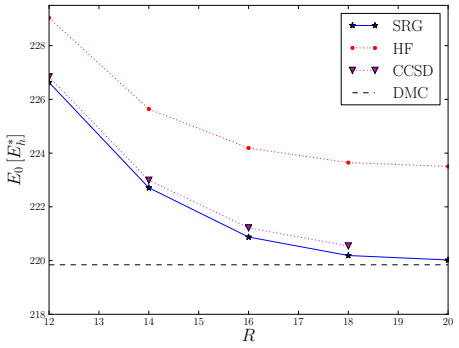

(c)Results for $N = 42$ and $\omega = 0.28$

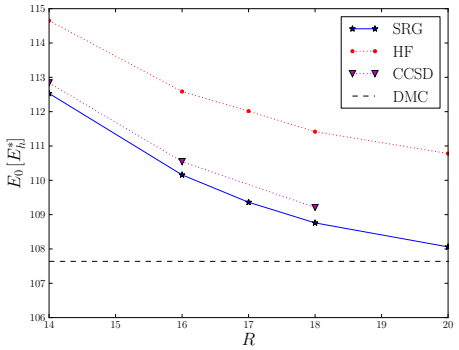

(d)Results for $N = 42$ and $\omega = 0.1$

FIG. 8. Comparison of our IM-SRG(2) ground state energies (SRG) for circular quantum dots for $N = 42$ and different values of ω. The results are compared with diffusion Monte Carlo (DMC), coupled cluster at the level of singles and doubles (CCSD), full configuration interaction (FCI) and Hartree-Fock calculations (HF) as functions of the number

TABLE I. Ground state energy (in atomic units) of a circular quantum dot, with N particles and oscillator frequency ω. The IM-SRG(2) results are given for $R = 20$ shells (except for the $N = 56$ results which are for $R = 18$), employing a Hartree-Fock basis, a bare Coulomb interaction and White's generator. For $N = 42$ and $\omega = 0.1$ results are presented up to $R = 22$ major shells. The results labelled IM-SRG(2)$_{R\to\infty}$ are obtained using the extrapolation formula of Eq.().

N	ω	IM-SRG(2)	IM-SRG(2)$_{R\to\infty}$	DMC
6	1.0	20.1583	20.1468	20.1593(1)
	0.5	11.7690	11.7631	11.7848(1)
	0.28	7.5713	7.5695	7.6002(1)
	0.1	3.4962	3.4977	3.5539(1)
12	1.0	65.7280	65.6990	65.7001(1)
	0.5	39.1631	39.1473	39.1596(1)
	0.28	25.6212	25.6140	25.6358(1)
	0.1	12.2223	12.2234	12.2698(1)
20	1.0	155.9737	155.9130	155.8822(1)
	0.5	93.9219	93.8853	93.8752(1)
	0.28	61.94362	61.9240	61.9268(1)
	0.1	29.95263	29.9565	29.9779(1)
30	1.0	308.7673	308.6053	308.5627(2)
	0.5	187.1671	186.8340	187.0426(2)
	0.28	124.0410	123.7171	123.9683(2)
	0.1	60.4319	60.1158	60.4205(2)
42	1.0	543.3398	543.3304	542.9428(8)
	0.5	330.8885	330.8425	330.6306(2)
	0.28	220.0226	219.9534y	219.8426(2)
	0.1	107.7851	106.8074	107.6389(2)
56	1.0	880.4159		879.3986(6)
	0.5	538.8199		537.353(2)
	0.28	360.83689		358.145(2)

MPPT does not do much better in the high frequency regimes as it often converges slower than IMSRG.

[[Q: should we discuss the absolute/relative correction plots?]]

For our addition and removal energy calculations, the results are summarized in Figure **??** and Figure **??** respectively. The figures show the the addition/removal energies for Hartree-Fock, combined with IM-SRG and/or QDPT (Hartree-Fock is always included, as usual) [[better way to explain this? the figure labels are somewhat misleading too]]. The DMC results are also shown via dashed lines where they are known.

From these results, we see that the QDPT corrections add a substantial contribution to the results of both Hartree-Fock with and without IM-SRG. [[quantify "substantial" numerically]]

For the IM-SRG results, there is a small asymmetry between the behavior of our removal and addition energies: we find that removal energies tend to be more accurate and its behavior is relatively stable with respect to the number of shells. [[why]]

Interestingly, the addition energy of Hartree-Fock with second-order QDPT appears to surpass the accuracy of that of IM-SRG with second-order QDPT. This is likely coincidental, as the third-order QDPT dramatically worsens the result.

Both Hartree-Fock and IM-SRG results worsen as the frequency decreases, which is not unexpected since the correlations become much more dominant. The Hartree-Fock appears to perform much worse, however, as the results converge much more slowly as the number of shells increases.

We also note that IM-SRG with 2 particles and frequency 0.1 generally fail to give any result as the ODE solver eventually leads to divergence [[Why?]] This seems to be a particular quirk associated with this specific system and does not usually occur in other systems except in a few extreme, isolated cases where there are far too few unoccupied states.

IV. CONCLUSIONS

We demonstrated the use various many-body theories, Hartree-Fock method, Møeller-Plesset perturbation theory, IM-SRG, as well as quasidegenerate perturbation theory to calculate ground state as well as addition and removal energies of two-dimensional quantum dots. We showed that these methods, when combined, can give a good approximate description of the systems at moderate cost compared to near-exact but much more expensive methods such as FCI and DMC.

For ground state energy, we showed that the convergence of IM-SRG is generally faster than that of MPPT, and the results are typically closer to the exact results. Similarly, we found that IM-SRG improves the rate of convergence of the addition and removal energies, both as the order of perturbation theory increases and as the number of shells increases.

There are several directions in which the calculations may be improved. One can attempt to improve the IM-SRG approximation by incorporating some of the missing higher-body terms in the commutator. This would also provide some insight into the rate of convergence with respect to the operator truncation. While some of the higher-body terms can be rather costly to compute – rendering a full 3-body IM-SRG quite expensive – certain additional approximations may be made to alleviate this without incurring the full cost of evolving 3-body operators [[Ref?]].

[[As noted earlier [[haven't written that yet]], the application of IM-SRG removes a large portion of the QDPT diagrams, which is beneficial as it increases the efficiency of the QDPT calculations. However, many of these diagrams can also be eliminated further through an infinite resummation scheme [[Any good refs for this?]], which would further reduce the number of diagrams in QDPT, especially those of lower order, whic would likely increase the accuracy of the result.]]

It would also be useful to investigate how the results obtained with finite number of shells in the basis are related to those obtained with an infinite number of shells in the basis. [[Ref: paper on IR/UV extrapolation]] With

a good theoretical foundation, a model of how the observables converge with respect to the size of the basis may be used to extrapolate the results to infinite-basis limit. This would also enable us to perform cheaper calculations with fewer shells and optimistically extrapolate results for large systems that would be otherwise infeasible to compute.

We note that this calculation was done entirely using the traditional approach of using a high-order ODE solver to solve the flow equation. A new technique developed by T. Morris [[Ref?]] uses an alternative approach that obviates the need for a high-order ODE solver, leading to much more efficient computations and also allowing operators of other observables to be evolved with greater ease. Implementing this approach would be beneficial as it would allows us to study the accuracy and convergence of other observables beyond energy and energy differences.

Implementation-wise, our current code constructs the two-particle basis as simple Slater determinants without any angular momentum coupling. This approach is often referred to as *m-scheme* in nuclear physics. This method is simple and works well for general systems, but it does not fully exploit the circular symmetry present in the quantum dot system. A more efficient approach is to use angular momentum coupling to generate the two-particle basis, which is known as *j-scheme* in nuclear physics. Combined with the symmetries of the Hamiltonian, this can significantly reduce the amount of computation required in this system, albeit at the cost of increasing the complexity of the implementation.

A more technical issue is its lack of parallelization: currently, the code makes very little use of parallelism and therefore does not scale well on modern clusters. As the problem is not embarrassingly parallel, implementing parallelism does introduce additional complications that must be considered. Distributing the workload across multiple nodes can significantly reduce the cost of the calculations, allowing larger systems to be studied.

ACKNOWLEDGMENTS

This work was supported by the National Science Foundation Grant No. PHY-1404159 (Michigan State University) and by the Research Council of Norway under contract ISP-Fysikk/216699.

[1] S. M. Reimann and M. Manninen, Rev. Mod. Phys. **74**, 1238 (2002).
[2] H.-A. Engel, V. N. Golovach, D. Loss, L. M. K. Vandersypen, J. M. Elzerman, R. Hanson, and L. P. Kouwenhoven, Phys. Rev. Lett. **93**, 106804 (2004).
[3] S. Tarucha, D. G. Austing, T. Honda, R. J. van der Hage, and L. P. Kouwenhoven, Phys. Rev. Lett. **77**, 3613 (1996).
[4] S. Strauf, K. Hennessy, M. Rakher, Y.-S. Choi, A. Badolato, L. C. Andreani, E. L. Hu, P. Petroff, and D. Bouwmeester, Phys. Rev. Lett. **96**, 127404 (2010).
[5] Z. Mi, J. Yang, P. Bhattacharya, G. Qin, and Z. Ma, Proceedings of the IEEE **97**, 1239 (2009).
[6] S. Jenks and R. Gilmore, Journal of Renewable and Sustainable Energy **2**, 013111 (2010).
[7] A. J. Nozik, M. C. Beard, J. M. Luther, M. Law, R. J. Ellingson, and J. C. Johnson, Chem. Rev. **110**, 6873 (2010).
[8] D. Loss and D. P. DiVincenzo, Phys. Rev. A **57**, 120 (1998).
[9] E. T. Ben-Ari, Journal of the National Cancer Institute **95**, 502 (2003).
[10] M. Taut, Phys. Rev. A **48**, 3561 (1993).
[11] A. D. Güçlü, J.-S. Wang, and H. Guo, Phys. Rev. B **68**, 035304 (2003).
[12] F. Pederiva, C. J. Umrigar, and E. Lipparini, Phys. Rev. B **62**, 8120 (2000).
[13] M. Pedersen Lohne, G. Hagen, M. Hjorth-Jensen, S. Kvaal, and F. Pederiva, Phys. Rev. B **84**, 115302 (2011).
[14] F. Bolton, Phys. Rev. B **54**, 4780 (1996).
[15] M. Eto, Japanese Journal of Applied Physics **36**, 3924 (1997).
[16] T. Ezaki, N. Mori, and C. Hamaguchi, Phys. Rev. B **56**, 6428 (1997).
[17] S. Kvaal, (2008).
[18] M. Rontani, C. Cavazzoni, D. Bellucci, and G. Goldoni, J. Chem. Phys. **124**, 124102 (2006).
[19] T. M. Henderson, K. Runge, and R. J. Bartlett, Phys. Rev. B **67**, 045320 (2003).
[20] I. Heidari, S. Pal, B. S. Pujari, and D. G. Kanhere, J. Chem. Phys. **127**, 114708 (2007).
[21] E. R. Anderson, S. K. Bogner, R. J. Furnstahl, and R. J. Perry, Phys. Rev. C **82**, 054001 (2010).
[22] S. K. Bogner, R. J. Furnstahl, and R. J. Perry, Phys. Rev. C **75**, 061001 (2007).
[23] O. Åkerlund, E. Lindgren, J. Bergsten, B. Grevholm, P. Lerner, R. Linscott, C. Forssen, and L. Platter, Eur. Phys. J. A **47**, 1 (2011).
[24] H. Hergert, S. K. Bogner, S. Binder, S. Calci, J. Langhammer, R. Roth, and A. Schwenk, Phys. Rev. C **78**, 014003 (2012).
[25] M. P. Lohne, *Coupled-cluster studies of quantum dots*, Master's thesis, University of Oslo (2010).
[26] S. Reimann, *Quantum-mechanical systems in traps and Similarity Renormalization Group theory*, Master's thesis, University of Oslo (2013).
[27] S. Kehrein, *The Flow Equation Approach to Many-Particle Systems*, Springer Tracts in Modern Physics (Springer, 2006).
[28] K. Tsukiyama, S. K. Bogner, and A. Schwenk, Phys. Rev. Lett. **106**, 222502 (2011).
[29] R. Roth, S. Binder, K. Vobig, A. Calci, J. Langhammer, and P. Navrátil, Phys. Rev. Lett. **109**, 052501 (2012).
[30] I. Shavitt and R. J. Bartlett, *Many-Body Methods in Chemistry and Physics: MBPT and Coupled-Cluster*

Theory, Cambridge Molecular Science (Cambridge University Press, 2009).
[31] R. J. Bartlett, Annu. Rev. Phys. Chem. **32**, 359 (1981).
[32] F. J. Wegner, Ann. Phys. **3**, 77 (1994).
[33] S. R. White, J. Chem. Phys. **117** (2002).
[34] B. Hammond, J. W. A. Lester, and P. J. Reynolds, *Monte Carlo Methods in Ab Initio Quantum Chemistry* (World Scientific Publishing Co., 1994).
[35] C. J. Umrigar, M. P. Nightingale, and K. J. Runge, J. of Chem. Phys. **99**, 2865 (1993).